JOURNAL OF APPLIED CRYSTALLOGRAPHY

Volume 54 (2021)

Supporting information for article:

DATAD: a Python-based X-ray diffraction simulation code for arbitrary texture and arbitrary deformation

J. W. Huang, Y. Y. Zhang, S. C. Hu, Y. Cai and S. N. Luo

Supplementary Information

DATAD: a Python-based X-ray Diffraction simulation code for Arbitrary Texture and Arbitrary Deformation

J. W. Huang,[a] Y. Y. Zhang,[a] S. C. Hu,[a] Y. Cai[a]* and S. N. Luo [b]*

[a] *The Peac Institute of Multiscale Sciences, Chengdu, Sichuan, P. R. China, and*

[b] *School of Materials Science and Engineering, Southwest Jiaotong University, Chengdu, Sichuan, P. R. China. E-mail: caiy@pims.ac.cn, sluo@swjtu.edu.cn*

1. Comparison of *DATAD* and some existing XRD simulation tools

Table S1: Comparison of the key features of *DATAD* and some existing XRD simulation tools

Tools	1D diffraction curve of ideal polycrystal specimens	2D diffraction pattern of single crystals	Near-field or far-field	Arbitrary strain	Arbitrary texture	Arbitrary X-ray spectra	Arbitrary diffraction geometry	User-friendly ODF handling
Mercury [a]	√	×	far-field	×	×	×	×	-
VESTA [b]	√	×	far-field	×	×	×	×	-
LaueX [c]	×	√	far-field	×	×	×	×	-
LAUEGEN [d]	×	√	far-field	×	×	×	×	-
LauePT [e]	×	√	far-field	×	×	×	×	-
Crystalsim [f]	×	√	far-field	×	×	×	×	-
XRDIFF [g]	×	√	far-field	×	×	×	×	-
LMGP [h]	×	√	far-field	×	×	×	×	-
PolyXSim [i]	√	√	far-field	√	√	×	×	×
Pagan *et al.* (2020)	√	√	far-field	√	√	√	×	×
Bernier *et al.* (2011)	×	√	far-field	√	√	×	×	×
QNFS [j]	×	√	near-field	×	√	×	×	-
Fang *et al.* (2020) [k]	×	√	near-field	√	√	√	×	×
GAPD with *ACAT* [l]	√	√	far-field	√	√	√	√	√
DATAD	√	√	far-field	√	√	√	√	√

[a] Macrae *et al.* (2006) [b] Momma & Izumi (2008) [c] Soyer (1996) [d] Campbell *et al.* (1998) [e] Huang (2010) [f] Kanagasabapathy (2016) [g] Weber (1997) [h] Laugier & Bochu (2001) [i] Sørensen (2008) [j] Knudsen (2009) [k] Fang *et al.* targets on cone-shaped laboratory X-ray source [l] *GAPD* (E *et al.*, 2018) and *ACAT* (Huang *et al.*, 2021) are based on atomic configurations.

2. Validation and application cases

We present below three validation and application cases, in terms of 1D and 2D diffraction patterns of a single crystal and two texture-free polycrystalline specimens (including a mixture) without or with applied uniaxial strain. In the discussion below, the coordinate system refers to the sample coordinate system, and length in a detection geometry is in arbitrary units, unless otherwise stated.

2.1. Single-crystal KCl of the B1 structure

The example code for simulating Laue diffraction of single-crystal KCl is shown in Fig. S1(a). A single-crystal KCl specimen of the B1 structure is constructed with its [100] and [001] crystallographic axes along the X- and Z-axes, respectively, and then rotated by 30° around the (1,1,1) axis. A white X-ray spectrum with photon energy ranging from 1 keV to 100 keV is used. The incident X-ray direction $\hat{v}_0$ is along the $-Z$-axis, and the transverse direction $\hat{t}$ is along the X-axis. A 30×30 planar detector is set perpendicular to the incident X-ray beam. The sample-to-PONI distance L is 20 and PONI is at the detector center.

(a)

```python
from datad import HKL, UnitCell, Pattern2D, SingleXtal, Detector, Xray
from numpy import linspace

unitcell_KCl = UnitCell.from_array((3.634, 3.634, 3.634, 90, 90, 90),
                                   (("K", (0, 0, 0)), ("Cl", (0.5, 0.5, 0.5)),), is_degree=True)
KCl = SingleXtal.from_miller_indices(unitcell_KCl, x=HKL(1, 0, 0), z=HKL(0, 0, 1), name="KCl")
xray = Xray.from_energy( linspace(1, 100, 500))
KCl.rotate_by_axis_angle(axis=(1, 1, 1), angle=30, is_degree=True)
p2d = Pattern2D(KCl, xray, inc=(0, 0, -1), vx=(1, 0, 0))
p2d.calc_peaks(sort_by="intensity")
detector = Detector(normal=(0, 0, 1), vx=(1, 0, 0), sizex=30, sizey=30, dist=20, ponix=15, poniy=15)
detector.project_peaks(p2d)
detector.calc_to_pic(sigmax=10, sigmay=10, ps=0.01)
detector.save_pic("KCl.tif")
```

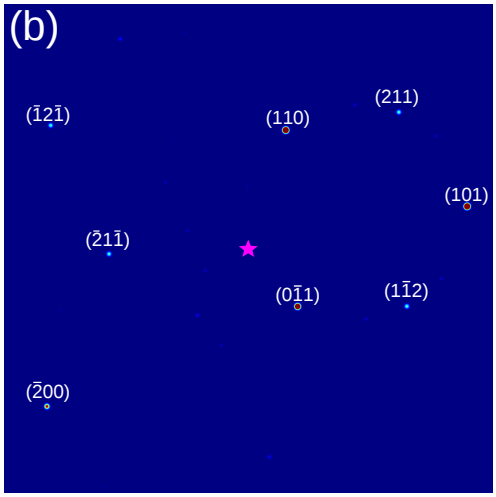

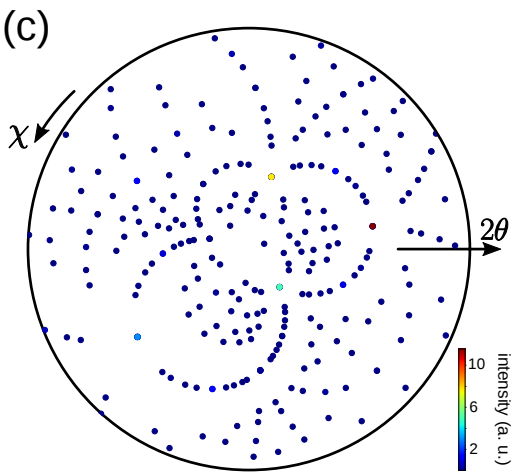

Fig. S1. Laue diffraction of single-crystal KCl of the B1 structure. (a) Example code. (b) 2D diffraction pattern on a planar detector. Pink star: direct beam. (c) Corresponding $\chi - 2\theta$ plot in the polar coordinate system.

The Laue diffraction pattern of the single-crystal KCl is shown on a planar detector (Fig. S1(b)) and in terms of the $\chi-2\theta$ plot in the polar coordinate system (Fig. S1(c)). For validation, the diffraction pattern is also simulated with *LauePT* (Huang, 2010) and the same parameters, and the positions and intensities of diffraction spots obtained from *DATAD* and *LauePT* are consistent.

2.2. Texture-free polycrystalline Fe under uniaxial strain

As shown in the example code in Fig. S2(a), a virtual texture-free, nonideal polycrystalline Fe specimen with 200,000 grains is constructed. Then a uniaxial strain of $\varepsilon_{xx} = -0.1$ is applied along the (1,1,1) axis. A narrow-band X-ray source with a central wavelength of 1.54 Å and a bandwidth of 0.2% is used here. The incident X-ray direction $\hat{v}_0$ and the transverse direction $\hat{t}$ are along the Z- and Y-axis, respectively. The diffraction pattern of the {110} planes is presented in Fig. S2(b) as an example.

(a)

```
from datad import NonidealPolyXtal, unitcell_Fe,\
  Xray, Pattern2D
from numpy import linspace

n = 200000
Fe = NonidealPolyXtal.uniform(unitcell_Fe, n)
Fe.strain1d(-0.1, axis=(1, 1, 1))
xray = Xray.from_wavelength(
  linspace(1.54 * 0.999, 1.54 * 1.001, 100))
p = Pattern2D(Fe, xray,
  inc=(0, 0, 1), vx=(0, 1, 0))
p.calc_peaks(max_tth=60, is_degree=True,
  sort_by="gamma")
p.save("Fe.txt")
```

(b)

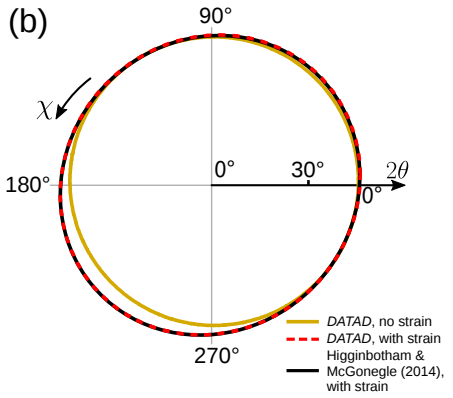

Fig. S2. (a) Example code that simulate the diffraction rings of strained Fe specimens. (b) $\chi - 2\theta$ plots in the polar coordinate system for strain-free and strained Fe specimens obtained from *DATAD* and Higginbotham & McGonegle (2014).

As shown in Fig. S2(b), the {110} Debye-Scherrer ring of the strain-free Fe specimen is perfectly circular. For the strained Fe specimen, the diffraction ring is distorted (quasi-elliptical), as a result of the nonhydrostatic components of the applied strain tensor; it is also off-center due to shear strains in the grains. The diffraction ring of the strained Fe specimen is also calculated following an analytical method of Higginbotham & McGonegle (2014). The analytical curve coincides with the simulated curve, providing another validation for *DATAD*.

2.3. Mixture of ideal polycrystalline Ta and Al

The parameters for simulating the 1D diffraction curve of a mixture of ideal polycrystalline Ta and Al are tabulated in Table S2. The corresponding example code is shown in Fig. S3(a). A Gaussian spectrum centered at 1.54 Å with a FWHM of 2.355% is used. The diffraction curve (Fig. S3(b)) is projected onto a tilted planar detector (Fig. S3(c)) and a cylindrical detector (Fig. S3(d)). The intensity variations on both detectors reflect the geometry effect in addition to that of structure factors.

Table S2. *Parameters used to simulate the Bragg diffraction of the mixture of ideal polycrystalline Ta and Al. Length is in arbitrary units unless stated otherwise.*

Diffraction	
central wavelength of X-ray spectrum	1.54 Å
FWHM of the spectrum	2.355%
incidence direction $\hat{v}_0$	(0, 0, −1)
transverse direction $\hat{t}$	(1, 0, 0)
Planar detector	
size	50 × 25
normal direction $\hat{n}$	(0.477, −0.477, 0.738)
direction of x_D axis	(0.869, 0.131, −0.477)
sample-to-PONI distance L	10
coordinates of PONI	(25, 12.5)
Cylindrical detector	
size	90 × 10
normal direction $\hat{n}$	(0, 0, 1)
direction of the x_D-axis	(1, 0, 0)
radius r	30
sample-to-PONI distance L	10
coordinates of PONI	(30, 5)
azimuthal angle ψ of origin O	5°

(a)

```python
from datad import unitcell_Ta, unitcell_Al, PolyXtal, Curve1D, Xray,  CylindricalDetector, Detector
Ta = PolyXtal(unitcell_Ta, name="Ta")
Al = PolyXtal(unitcell_Al, name="Al")
xray = Xray.Gaussian(1.54, 1.54 * 0.01)
p1d = Curve1D((Ta, Al), xray)
p1d.calc_peaks(min_tth=30, max_tth=115, is_degree=True, sort_by="tth")
det1 = Detector(normal=(0, 0, 1), vx=(1, 0, 0), sizex=50, sizey=25, dist=10, ponix=25, poniy=25 / 2)
det1.rotate_by(axis=(1, 1, 0), angle=30, is_degree=True)
det1.project_peaks(p1d)
det1.calc_to_pic(tth_res=0.08, ps=0.01, is_degree=True)
det1.save_pic("det1.tif")
det2 = CylindricalDetector(normal=(0, 0, 1), vx=(1, 0, 0), sizex=90, sizey=10, dist=10,
                           ponix=30, poniy=5, radius=30, start_angle=5)
det2.project_peaks(p1d)
det2.calc_to_pic(tth_res=0.08, ps=0.01, is_degree=True)
det2.save_pic("det2.tif")
```

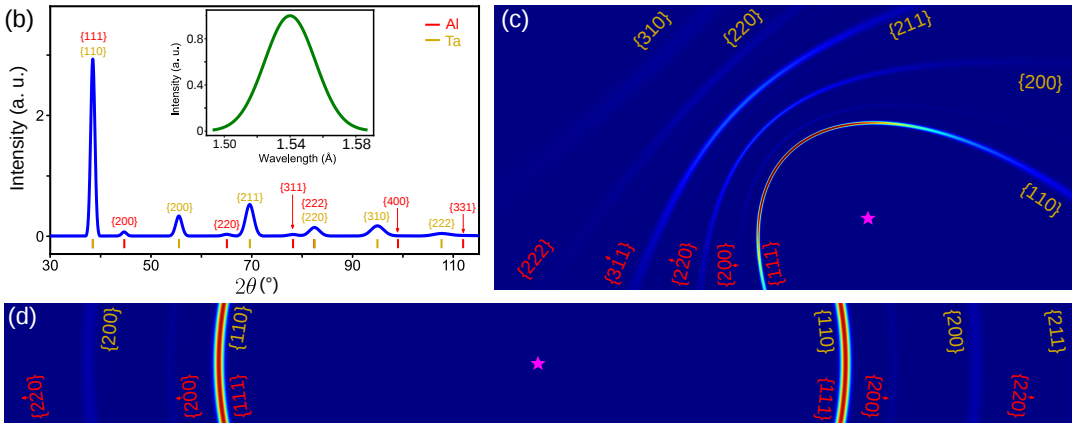

Fig. S3. Bragg diffraction of a mixture of ideal polycrystalline Ta and Al. (a) Example code. (b) 1D diffraction curve. Inset: X-ray spectrum. (c) 2D diffraction pattern projected on a planar detector. (d) 2D diffraction pattern projected on a cylindrical detector (expanded).

References

Bernier, J. V., Barton, N. R., Lienert, U. & Miller, M. P. (2011). *The Journal of Strain Analysis for Engineering Design*, **46**(7), 527–547.

Campbell, J., Hao, Q., Harding, M., Nguti, N. & Wilkinson, C. (1998). *Journal of Applied Crystallography*, **31**(3), 496–502.

E, J. C., Wang, L., Chen, S., Zhang, Y. Y. & Luo, S. N. (2018). *Journal of Synchrotron Radiation*, **25**(2), 604–611.

Fang, H., Juul Jensen, D. & Zhang, Y. (2020). *Acta Crystallographica Section A: Foundations and Advances*, **76**(6).

Higginbotham, A. & McGonegle, D. (2014). *Journal of Applied Physics*, **115**(17), 174906.

Huang, J. W., Cai, Y., Zhong, Z. Y. & Luo, S. N. (2021). *Computational Materials Science*, **186**, 109997.

Huang, X. R. (2010). *Journal of Applied Crystallography*, **43**(4), 926–928.

Kanagasabapathy, M., (2016). Crystalsim - xrd hkl simulation software.

Knudsen, E. B., (2009). *Quasi-nearfield simulator.*
URL: *https://sourceforge.net/p/fable/wiki/nearfield-simulation/*

Laugier, J. & Bochu, B., (2001). *LMGP.*
URL: *http://www.ccp14.ac.uk/tutorial/lmgp/*

Macrae, C. F., Edgington, P. R., McCabe, P., Pidcock, E., Shields, G. P., Taylor, R., Towler, M. & Streek, J. (2006). *Journal of Applied Crystallography*, **39**(3), 453–457.

Momma, K. & Izumi, F. (2008). *Journal of Applied Crystallography*, **41**(3), 653–658.

Pagan, D. C., Jones, K. K., Bernier, J. V. & Phan, T. Q. (2020). *JOM*, pp. 1–12.

Sørensen, H. O., (2008). *PolyXSim.*
URL: *https://github.com/FABLE-3DXRD/PolyXSim*

Soyer, A. (1996). *Journal of Applied Crystallography*, **29**(4), 509–509.

Weber, S. (1997). *Journal of Applied Crystallography*, **30**(5), 565–566.